

Research  
Report

## Ultrahigh-quality Silicon Carbide Single Crystals

Daisuke Nakamura, Itaru Gunjishima, Satoshi Yamaguchi, Tadashi Ito,  
Atsuto Okamoto, Hiroyuki Kondo, Shoichi Onda, Kazumasa Takatori

---

### Abstract

Silicon carbide (SiC) has a range of useful physical, mechanical and electronic properties that make it a promising material for next-generation electronic devices.<sup>1, 2)</sup> Careful consideration of the thermal conditions<sup>3-6)</sup> in which SiC {0001} is grown has resulted in improvements in crystal diameter and quality: the quantity of macroscopic defects such as hollow core dislocations (micropipes),<sup>7-9)</sup> inclusions, small-angle boundaries and long-range lattice warp has been reduced.<sup>10, 11)</sup> But some macroscopic defects (about 1-10 cm<sup>-2</sup>) and a large density of elementary dislocations ( $\sim 10^4$  cm<sup>-2</sup>),

such as edge, basal plane and screw dislocations, remain within the crystal, and have so far prevented the realization of high-efficiency, reliable electronic devices in SiC (Refs. 12-16). Here we report a method, inspired by the dislocation structure of SiC grown perpendicular to the *c*-axis (*a*-face growth),<sup>17)</sup> to reduce the number of dislocations in SiC single crystals by two to three orders of magnitude, rendering them virtually dislocation-free. These substrates will promote the development of high-power SiC devices and reduce energy losses of the resulting electrical systems.

Keywords

Semiconductor, Silicon carbide, Single crystal, Power device, Crystal growth, Dislocation

---

## 1. Introduction

---

Single crystals of the conventional electronic materials silicon and gallium arsenide are grown dislocation-free from molten sources by means of the 'necking' process.<sup>18, 19)</sup> But SiC single crystals are usually produced by a gas-phase growth method<sup>20)</sup> in which the necking process is not suitable, because rapid increase of crystal diameter is impossible.

Once grown, a single crystal of SiC is usually produced by means of *c*-face growth, which involves growing the crystal along the  $\langle 0001 \rangle$  (*c*-axis) direction using a seed of  $\{0001\}$  substrate within an offset angle about  $10^\circ$ . The generation of defects in a *c*-face-growth crystal is considerably affected by defects in the seed crystal. Thus, it is crucial not only to optimize the growth conditions but also to reduce the dislocations in the seed crystal. We have noticed the particular dislocation structure of SiC single crystal obtained by *a*-face growth,<sup>17)</sup> and this is the key to solving the problem. In this Letter, both  $\{11\bar{2}0\}$  and  $\{1\bar{1}00\}$  faces are called '*a*-face', and both  $\langle 11\bar{2}0 \rangle$  and  $\langle 1\bar{1}00 \rangle$  axes are called '*a*-axis', because the dislocation structures of crystal grown along both  $\langle 11\bar{2}0 \rangle$  and  $\langle 1\bar{1}00 \rangle$  directions are almost the same (strictly speaking, *a*-axis is not  $\langle 1\bar{1}00 \rangle$  but  $\langle 11\bar{2}0 \rangle$ ).

---

## 2. Dislocation structure of crystals grown perpendicular to *c*-axis

---

First, we investigated the X-ray incident angle ( $\omega$ ) scan rocking curves of the 0004 diffraction peak spectrum obtained from 4H-SiC  $\{0001\}$  substrate; the substrate was sliced from an *a*-face  $\{1\bar{1}00\}$  growth ingot obtained using a *c*-face growth seed crystal. From this analysis, we found that *c*-axis perturbation parallel to the growth direction is much smaller than that perpendicular to the growth direction. The width of the peak spectrum (full-width at half-maximum, FWHM, 27 arcsec), which was obtained in the case that the  $\omega$ -scan axis is perpendicular to the growth direction (case A), almost equalled that of perfect crystal (26 arcsec) in our apparatus, indicating that there is little perturbation in the direction parallel to the growth direction of *a*-face growth crystal. On the other

hand, the FWHM of the peak which was obtained where the  $\omega$ -scan axis is parallel to the growth direction (case B) was much broader.<sup>17)</sup> We surmise that anisotropy with regard to the crystallographic axis perturbation is peculiar to *a*-face growth of hexagonal crystals. Moreover, we found that the FWHM (in case B) plots for various measurement points *z*, which is the distance from seed crystal in the direction parallel to the growth direction, does not change as a function of *z*. In other words, *a*-face growth crystal faithfully inherits only the *c*-axis variations perpendicular to the growth direction. We call the resultant crystal lattice distortion a 'corrugated plate' lattice.

From these results, we propose that most of dislocations in *a*-face growth SiC single crystals exist almost parallel to the growth direction with the Burgers vectors perpendicular and parallel to the growth direction, and the density of dislocations hardly changes at all with changes in growth height. That is, the 'corrugated plate' lattice is due to a high density of edge dislocations parallel to the growth direction. X-ray topographic analysis found that many edge dislocations exist parallel to the growth direction, and so has confirmed that this model is appropriate. The same result was obtained with the **g** vector being 0004 as with  $11\bar{2}0$ , which the **g** vector is diffraction vector. These results are consistent with our model of dislocation structure. In addition, almost the same results were obtained from another *a*-face growth crystal- $\{11\bar{2}0\}$ , perpendicular to  $\{1\bar{1}00\}$ .

---

## 3. Repeated *a*-face growth process

---

We attempted to reduce dislocations by utilizing *a*-face growth and the dislocation structure of an *a*-face growth crystal. The process to eliminate dislocations is as follows. Step 1: *a*-face ( $\{11\bar{2}0\}$  or  $\{1\bar{1}00\}$ ) growth along the *a*-axis ( $\langle 11\bar{2}0 \rangle$  or  $\langle 1\bar{1}00 \rangle$ ) direction, using a seed sliced from a *c*-face growth ingot. Step *N* (*N* = 2, 3, 4,...): *a*-face ( $\{1\bar{1}00\}$  or  $\{11\bar{2}0\}$ ) growth along the *a*-axis ( $\langle 1\bar{1}00 \rangle$  or  $\langle 11\bar{2}0 \rangle$ ) direction, using a seed sliced from the *a*-face growth ingot of the previous step (step *N*-1): the seed surface orientation is perpendicular to both the previous step's growth and  $\langle 0001 \rangle$  directions. Step *N*+1: *c*-face growth, using a seed sliced from the *a*-

face growth ingot of the previous step (step  $N$ ): the seed surface orientation is  $\{0001\}$ , with several degrees off-axis towards the perpendicular to both the previous step's growth and  $\langle 0001 \rangle$  directions.

We call this the 'repeated  $a$ -face' (RAF) growth process, because the steps of repeated  $a$ -face growth are crucial. To simplify, we here explain the case of  $N = 2$  (Fig. 1a), where  $N$  is a repeat count of  $a$ -face

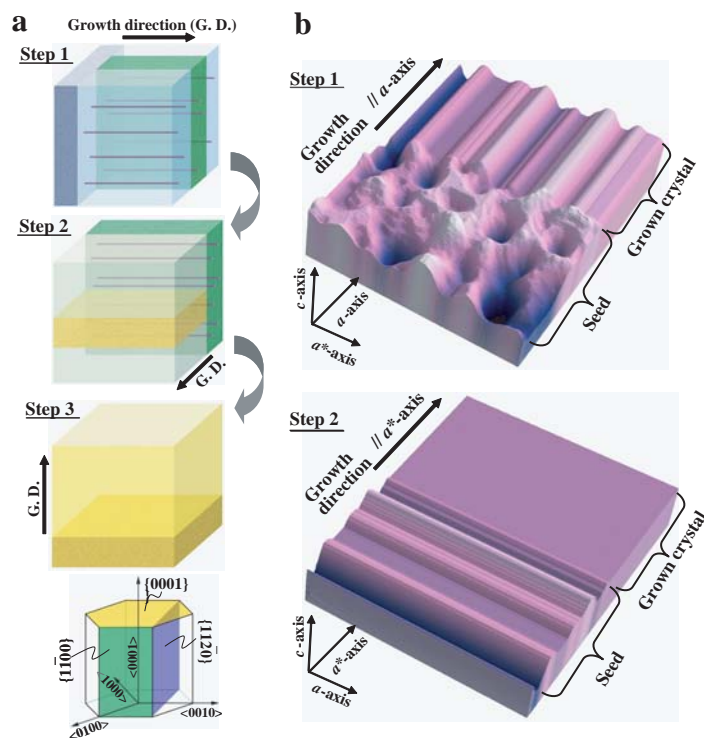


**Fig. 1** Schematic illustrations of 'repeated  $a$ -face' (RAF) growth process. The growth sequences are as follows. Step 1: first  $a$ -face growth (seed and grown crystal are shown dark blue and light blue, respectively). GD, growth direction. Step 2: second  $a$ -face growth perpendicular to first  $a$ -face growth (seed sliced from first  $a$ -face growth crystal, and the grown crystal are shown dark green and light green, respectively). Step 3:  $c$ -face growth with offset angle of several degrees (seed sliced from second  $a$ -face growth crystal, and the grown crystal are shown dark yellow and light yellow, respectively) **a**. In this figure, the first and second  $a$ -faces are  $\{11\bar{2}0\}$  and  $\{1\bar{1}00\}$  faces. At the bottom of panel **a** are shown the major crystallographic axes and lattice planes in the RAF process. Dislocation characteristic of  $a$ -face growth crystal (first  $a$ -face growth crystal and second seed crystal of panel **a**) is shown by purple line. **b**, Top side view, showing  $\{0001\}$  lattice plane irregularities of seed and grown crystal in steps 1 and 2. The  $a^*$ -axis is perpendicular to both the  $a$ -axis and the  $c$ -axis.

growth. In step 1, we can obtain a crystal with a high density of dislocations, which are inherited from the crude seed crystal, parallel to the growth direction. In step 2, most of the dislocations are not exposed to a surface of the second seed, because most of the dislocations exist perpendicular to the first  $a$ -face growth direction, that is, parallel to the second seed surface. Therefore, the second  $a$ -face growth crystal inherits fewer dislocations, and we can obtain a crystal with much lower dislocation density. In addition, it may be seen that we can reduce the dislocation density further by increasing the repeat count  $N$ . In step 3, we have to eliminate stacking faults<sup>17)</sup> due to  $a$ -face growth in the step 2 growth crystal. We can eliminate such faults by  $c$ -face growth, because the stacking faults and partial dislocations accompanying them are inherited only perpendicular to the  $c$ -axis. Moreover, we can reduce the inheritance of dislocations by using a seed with several degrees off-axis towards the perpendicular to both second  $a$ -face growth and  $\langle 0001 \rangle$  directions, because most of the remaining dislocations in the second  $a$ -face growth crystal are parallel to the third seed surface. In addition, an offset angle of several degrees is needed to achieve polytype stability.<sup>21)</sup>

#### 4. Results and discussion

Figure 1b is a schematic illustration of crystal lattice plane distortion. The  $\{0001\}$  lattice plane of  $c$ -face growth crude seed crystal is ridged randomly. However, that of the first  $a$ -face (step 1) growth crystal is like 'corrugated plate' because  $a$ -face growth crystal inherits only the  $c$ -axis perturbation perpendicular to the growth direction from the crude seed crystal surface. Finally, the  $\{0001\}$  lattice plane of the second  $a$ -face (step 2) growth crystal is very flat (in other words, the lattice distortion accompanied with a lot of dislocations is eliminated), because there is little perturbation inherited from the first  $a$ -face growth seed surface. By experiment, we confirmed that the FWHM values of X-ray rocking curves obtained from second  $a$ -face growth crystal in both case A and case B were almost equal to each other, both being uniformly low. Moreover, long-range warp of the lattice plane was eliminated with the elimination of

*c*-axis perturbation.

**Figure 2** shows plots of averaged etch pit density (EPD) of 4H-SiC (0001)  $8^\circ$  off-axis substrates obtained by the RAF process. The repeat count value of zero refers to the *c*-face growth crude crystal. Repeat counts one, two and three refer respectively to the ' $\{1\bar{1}00\}$  and *c*-face', ' $\{1\bar{1}00\}$  and  $\{11\bar{2}0\}$  and *c*-face' and ' $\{1\bar{1}00\}$  and  $\{11\bar{2}0\}$  and  $\{1\bar{1}00\}$  and *c*-face' growth crystal in the RAF process. As shown clearly in Fig. 2, the EPD decreases exponentially with increase in the repeat count of *a*-face growth. This shows that dislocations in the SiC crystal are effectively eliminated by the RAF growth. Moreover, we confirmed by successive etch pit patterns and X-ray topographies that the stacking faults and partial dislocations exposed on the RAF seed surfaces are eliminated perfectly by the *c*-face growth because the stacking faults and partial dislocations propagate only along the  $\{0001\}$  plane. The average EPD and micropipe density of a 20-mm-diameter substrate, taken from

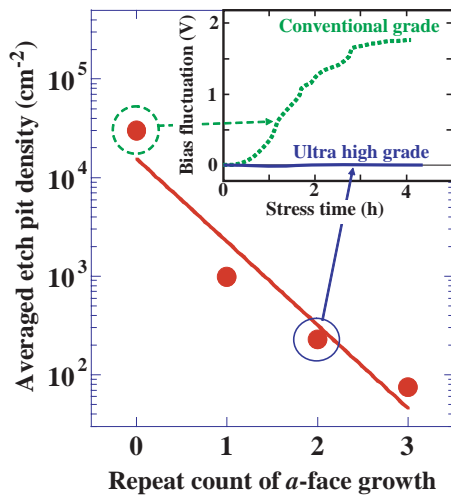


**Fig. 2** Etch pit density (EPD) decay curves versus repeat count of *a*-face growth, and results of current stress testing. Each averaged EPD was calculated from the results of 90 observation points within a range 20 mm in diameter. The inset shows forward bias fluctuation of PiN diodes under the stress with a constant current density. The broken green line is that of crude substrate<sup>22)</sup> with a current density of 160 A cm<sup>-2</sup>, and the solid blue line is that of RAF substrate with 300 A cm<sup>-2</sup>.

the crystal grown on RAF seed with *a*-face growth performed three times (Fig. 2), were respectively 75 cm<sup>-2</sup> and 0 cm<sup>-2</sup>. This EPD value is lower by three orders of magnitude than that of conventional grade SiC substrates. We think that a repeat count of *a*-face growth greater than three will lead to a lower EPD value and a higher crystal quality; the experiments are now under way. In addition, we have investigated current-induced degradation of PiN devices fabricated on the RAF substrate. As shown in an inset of Fig. 2, only a little fluctuation is observed in forward bias (<15 mV) on the ultrahigh-quality RAF substrate, whereas a rapid increase occurs in the bias on the conventional grade substrate.<sup>22)</sup> This means that the reliability of bipolar devices is much enhanced by the RAF process.

Next, we attempted to enlarge the crystal diameter by the RAF process. From the standpoint of crystal growth, the enlargement of crystal size give rise to various problems. In the case of SiC crystal growth, the effects of thermal stress and foreign polytype inclusion are most crucial. To maintain good crystal quality under crystal growth, we have optimized the crucible structures, growth conditions and seed positioning method, and have managed both enlargement and quality. As a result, we have obtained large RAF substrates, 1.5-3.0 inches in diameter, whose averaged EPDs were lower by about two orders of magnitude than these of conventional SiC substrates. We have evaluated the crystal quality of the large RAF substrate by synchrotron monochromatic beam X-ray topography (**Fig. 3**). As shown in Fig. 3a, crystal quality of the RAF substrate is very homogeneous, and there are very few macroscopic defects and dislocations; we also found that the long-range lattice warp is very small, with the curvature radius of the lattice evaluated to be about 800 m. On the other hand, as shown in Fig. 3b, conventional grade substrate has many macroscopic defects and dislocation networks.

## 5. Conclusion

The crystal quality of RAF substrates is much better than that of conventional substrates; we have shown that the RAF growth process is very effective in reducing dislocations and other defects.



Moreover, we have succeeded in manufacturing a large size substrate by this method, which makes feasible commercial applications. We consider that it will be possible in the near future to eliminate dislocations perfectly, and to enlarge the diameter to several inches. Finally, we suggest that the concept of the RAF process can be applied to single-crystal growth of other materials that have hexagonality in their crystal structures.

### Methods

#### EPD evaluation by molten KOH etching

EPDs have been considered to be the density of dislocations exposed at the substrate surface. The molten KOH etching was performed at 773 K for 20-30 min in a nickel crucible. After the etching, etch pits were observed by optical microscopy. The field of view at each observation point was  $870 \times 650 \mu\text{m}$ . The observation points were located in

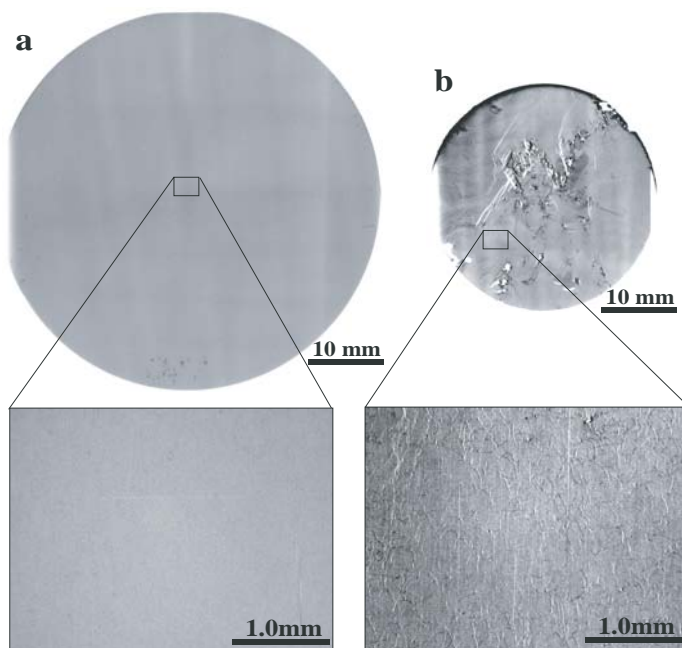


**Fig. 3** Synchrotron monochromatic beam X-ray topographies. 4H-SiC (0001)  $8^\circ$  off-axis substrate, 2.0 inches in diameter, manufactured by the RAF process (a) and a 1.2-inch-diameter specimen manufactured by the conventional process (only *c*-face growth; b). Averaged EPD and micropipe density of the RAF growth crystal were about  $250 \text{ cm}^{-2}$  and  $0 \text{ cm}^{-2}$ , respectively, and those of crystal grown by the conventional method were about  $3 \times 10^4 \text{ cm}^{-2}$  and  $30 \text{ cm}^{-2}$ , respectively. Enlarged images are shown below. Dislocation networks are shown in the enlarged image of b.

tetragonal grids, and the distance between each point was 2.0 or 3.0 mm.

### Synchrotron monochromatic beam X-ray topography

The experiment was done at SPring-8 (BL20-B2). The topographies were taken with Berg-Barrett geometry with the diffraction plane of  $11\bar{2}\bar{8}$ . Incident X-ray energy was 11.94 keV, and immersion depth of reflection beam was about  $4 \mu\text{m}$ . The topographies in Fig. 3 were obtained by continuous scan of incident angle ( $\omega$ ), and the zebra patterns to evaluate the curvature radius of crystal lattice planes were taken by step scan of that. Dislocations in the topography appear as black or white lines or dots.

### References

- 1) Bhatnagar, M. and Baliga, B. J. : "Comparison of 6H-SiC, 3C-SiC, and Si for power devices", IEEE Trans. Electron Devices, **40**(1993), 645-655
- 2) Harris, C. I., Savage, S., Konstantinov, A., Bakowski, M. and Ericsson, P. : "Progress towards SiC products", Appl. Surf. Sci., **184**(2001), 393-398
- 3) Yakimova, R., et al. : "Seeded sublimation growth of 6H and 4H-SiC crystals", Mater. Sci. Eng. B, **61/62**(1999), 54-57
- 4) Selder, M., Kadinski, L., Durst, F. and Hofmann, D. : "Global modeling of the SiC sublimation growth process: prediction of thermoelastic stress and control of growth conditions", J. Cryst. Growth, **226**(2001), 501-510
- 5) Kato, T., et al. : "In-situ observation of silicon carbide sublimation growth by X-ray topography", J. Cryst. Growth, **222**(2001), 579-585
- 6) Oyanagi, N., Yamaguchi, H., Kato, T., Nishizawa, S. and Arai, K. : "Growth and evaluation of high quality SiC crystal by sublimation method", Mater. Sci. Forum, **389/393**(2002), 87-90
- 7) Frank, F. C. : "Capillary equilibria of dislocated crystals", Acta Crystallogr, **4**(1951), 497-501
- 8) Heindl, J., et al. : "Dislocation content of micropipes in SiC", Phys. Rev. Lett., **80**(1998), 740-741
- 9) Gutkin, M. Yu., et al. : "Synchrotron radiographic study and computer simulation of reactions between micropipes in silicon carbide", J. Appl. Phys., **94**(2003), 7076-7082
- 10) Muller, St. G., et al. : "High quality SiC substrates for semiconductor devices: from research to industrial production", Mater. Sci. Forum, **389/393**(2001), 23-28
- 11) Muller, St. G., et al. : "Sublimation-grown semi-insulating SiC for high frequency devices", Mater. Sci. Forum, **433/436**(2003), 39-44
- 12) Neudeck, P. G., Huang, W. and Dudley, M. :

- "Breakdown degradation associated with elementary screw dislocations in 4H-SiC p+n junction rectifiers", Solid-State Electron., **42**(1998), 2157-2164
- 13) Lendenmann, H., et al. : "Long term operation of 4.5kV PiN and 2.5kV JBS diodes", Mater. Sci. Forum, **353/356**(2001), 727-730
- 14) Malhan, R. K., Nakamura, H., Onda, S., Nakamura, D and Hara, K. : "Impact of SiC structural defects on the degradation phenomenon of bipolar SiC devices", Mater. Sci. Forum, **433/436**(2003), 917-920
- 15) Senzaki, J., Kojima, K. and Fukuda, K. : "Long-term reliability of n-type 4H-SiC thermal oxides (3)", In Extended Abstracts of the 51st Spring Meeting of the JSAP, Vol. 1(2004), 433, Jpn. Soc. Appl. Phys., Tokyo [in Japanese]
- 16) Tanimoto, S., et al. : "Impact of surface crystal-defects on TDDDB event of SiC thermal oxide", In Extended Abstracts of the 51st Spring Meeting of the JSAP, Vol.1(2004), 434, Jpn. Soc. Appl. Phys., Tokyo [in Japanese]
- 17) Takahashi, J., Ohtani, N., Katsuno, M. and Shinoyama, S. : "Sublimation growth of 6H- and 4H-SiC single crystals in the  $[1\bar{1}00]$  and  $[11\bar{2}0]$  directions", J. Cryst. Growth, **181**(1997), 229-240
- 18) Dash, W. C. : "Growth of silicon crystals free from dislocations", J. Appl. Phys., **30**(1959), 459-474
- 19) Zulehner, W. : "Historical overview of silicon crystal pulling development", Mater. Sci. Eng. B, **73**(2000), 7-15
- 20) Tairov, Y. M. and Tsvetkov, V. F. : "Investigation of growth processes of ingots of silicon carbide single crystals", J. Cryst. Growth, **43**(1978), 209-212
- 21) Matsunami, H. and Kimoto, T. : "Step-controlled epitaxial growth of SiC: High quality homoepitaxy", Mater. Sci. Eng., **R20**(1997), 125-166
- 22) Stahlbush, R. E., et al. : "Propagation of current-induced stacking faults and forward voltage degradation in 4H-SiC PiN diodes", Mater. Sci. Forum, **389/393**(2002), 427-430

Reprinted with permission from NGP Nature Asia Pacific (Nature, 430-7003(2004), 1009-1012).



#### Daisuke Nakamura

Research fields : Material science  
( Inorganic materials,  
Semiconductor, Crystal growth)  
Academic society : Jpn. Soc. Appl. Phys.  
Awards : Young Scientist Award for the  
Presentation of an Excellent paper,  
2005 (Jpn. Soc. Appl. Phys.)



#### Itaru Gunjishima

Research fields : Carbonic materials,  
Single crystals  
Academic degree : Dr. Eng.  
Academic society : Ceram. Soc. Jpn.



#### Satoshi Yamaguchi

Research fields : Material analysis using  
synchrotron radiation  
Academic society : Jpn. Soc. Synchrotron  
Radiation Res.



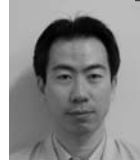
#### Tadashi Ito

Research fields : Silicon and related  
semiconductor thin film solar cells,  
Purification of metallic grade  
silicon to solar cell grade silicon.  
Academic degree : Dr. Eng.  
Academic society : Inst. Electr. Eng. Jpn.,  
Jpn. Soc. Appl. Phys.,  
Meteorological Soc. Jpn.



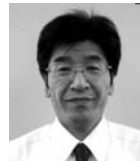
#### Atsuto Okamoto

Research fields : Material science  
(Inorganic materials, Nanocarbons)  
Academic society : Jpn. Soc. Appl. Phys.,  
Jpn. Assoc. Cryst. Growth Co.,  
Carbon Soc. Jpn., Fullerene-  
Nanotubes Re. Assoc.  
Awards : The 32nd National Conf. of  
Cryst. Growth Incentive Award,  
2002



#### Hiroyuki Kondo\*

Research fields : Research and  
development of silicon carbide  
single crystal growth  
Academic society : Jpn. Soc. Appl. Phys.



#### Shoichi Onda\*

Research fields : Development of wafers  
and power devices of silicon  
carbide, Development of silicon-  
carbide-based inverter system  
Academic society : Jpn. Soc. Appl. Phys.



#### Kazumasa Takatori

Research fields : Inorganic material  
Academic degree : Dr. Eng.  
Academic society : Ceram. Soc. Jpn.

\*DENSO Corp. Res. Labs.